Materiales de Construcción 75 (358)
April-June 2025, e377
ISSN-L: 0465-2746, eISSN: 1988-3226
https://doi.org/10.3989/mc.2025.395824

Lightweight gypsum composite material to improve energy efficiency: Assessment of physico-chemical, mechanical, thermal and fire performance properties

A. Zaragoza-Benzal [a] ✉, D. Ferrández [a], P. Santos [b], E. Atanes-Sánchez [c]

a. Building Technology Department, Polytechnic University of Madrid (Madrid, Spain)
b. University of Coimbra, ISISE, ARISE Department of Civil Engineering, (Coimbra, Portugal)
c. Department of Mechanical Engineering, Chemical and Industrial Design, Polytechnic University of Madrid (Madrid, Spain)
✉: alicia.zaragoza@upm.es

Received 6 October 2024
Accepted 22 December 2024
Available on line 19 September 2025

ABSTRACT: This study addresses the development of a new composite material made under circular economy criteria using natural and recycled resources. Recycled expanded polystyrene is innovatively integrated into the matrix of gypsum-based materials reinforced with fibers. This approach has progressively reduced the consumption of raw materials up to 18.2%, resulting in a reduction of 31.7% in density. This results in a reduction of 47.2% thermal conductivity compared to conventional gypsum and an improvement in the energy efficiency of the construction systems, increasing their thermal resistance by up to 21.1%. Additionally, the mechanical characterization results comply with the minimum regulated requirements. Physico-chemical characterization and material's microstructure analysis were also conducted. Finally, an assessment of the material's behavior under fire conditions is included, analyzing the hazard emissions released. This study contributes to the development of new sustainable construction materials to produce more energy-efficient prefabricated products.

KEY WORDS: Construction material; Thermal behavior; Energy efficiency; Physico-chemical characterization; Fire performance.

Citation/Citar como: Zaragoza-Benzal A, Ferrández D, Santos P, Atanes-Sánchez E. 2025. Lightweight gypsum composite material to improve energy efficiency: Assessment of physico-chemical, mechanical, thermal and fire performance properties. Mater. Construcc. 75(358):e377. https://doi.org/10.3989/mc.2025.395824

RESUMEN: *Compuesto de yeso aligerado para mejorar la eficiencia energética: Evaluación de las propiedades fisicoquímicas, mecánicas, térmicas y de comportamiento frente al fuego.* En este estudio se desarrolla un nuevo compuesto fabricado bajo criterios de economía circular utilizando recursos naturales y reciclados. El poliestireno expandido reciclado se integra de forma innovadora en compuestos de yeso reforzados con fibras. Este enfoque ha permitido reducir el consumo de materias primas hasta un 18,2%, reduciendo su densidad en un 31,7%. Así mismo, se ha obtenido la disminución del 47,2% en la conductividad térmica en comparación con el yeso convencional y un aumento de la resistencia a térmica de los sistemas de construcción del 21.1%. Además, los resultados de la caracterización mecánica cumplen los requisitos mínimos normativos. También se realizó una caracterización físico-química y el análisis microestructural del material. Por último, se incluye una evaluación del comportamiento del material ante el fuego, analizando las emisiones tóxicas liberadas. Este estudio contribuye al desarrollo de nuevos materiales de construcción sostenibles para la fabricación de productos prefabricados más eficientes energéticamente.

PALABRAS CLAVE: Material de construcción; Comportamiento térmico; Eficiencia energética; Caracterización fisicoquímica; Comportamiento frente al fuego.

1. INTRODUCTION

The European Green Deal sets among its objectives the reduction of greenhouse gas emissions by 55% by 2030, aiming to achieve carbon neutrality by 2050 (1). This entails establishing a network of buildings with near-zero consumption and emissions by adopting measures to improve energy efficiency and incorporating circular economy models (2). However, these goals are far from being achieved, with buildings accounting for 36% of total atmospheric CO_2 emissions and consuming 40% of the total energy produced (3). In this context, the development of new, more efficient and less polluting building materials and construction systems represents one of the greatest challenges for European society today.

With the industrialization of construction and the rise of prefabricated systems, gypsum-based materials are emerging as a sustainable alternative for the manufacture of modular construction components (4). The sustainability of gypsum material is due to its virtually infinite recycling process (5), its production as by-product in many industrial processes (6), and its non-structural applications which allow for a greater incorporation of secondary raw materials into its matrix (7). Consequently, in recent decades, several researchers have sought to improve the thermal performance of gypsum materials by incorporating waste from thermal insulation materials (8). Among these, expanded polystyrene (EPS) has been widely used as an addition in different proportions, as shown in Table 1, which summarizes the studies conducted in the last five years.

Table 1. Literature review (2020-2024): gypsum-based materials with EPS addition.

Reference (year)	Addition	Added quantity	Other additions	(kg/m^3)	(W/m·K)
(9) (2020)	EPS waste triturated	25% – 50% by volume	Ceramic aggregates	1030 – 1170	0.28 – 0.35
(10) (2021)	EPS waste granules	5% – 30% by mass	—	960 – 730	0.16 – 0.28
(11) (2021)	EPS granules	15% – 60% by volume	Cellulose fiber	372 – 513	0.18 – 0.29
(12) (2022)	EPS slurry	14.3% – 50.5% by mass	—	1925 – 2287	0.23 – 0.28
(13) (2023)	EPS granules	1.7% by mass	—	730	—
(14) (2023)	EPS granules	4% by mass	—	295 – 793	0.13 – 0.25
(15) (2023)	EPS solution	8.9% – 26.5% by mass	—	746 – 944	0.08 – 0.18
(16) (2023)	EPS waste triturated	10% – 80% by volume	—	1240 – 420	0.11 – 0.38
(7) (2024)	EPS waste triturated	0.5% - 1.5% by mass	Paper and Polyester	718 - 810	0.25 – 0.32
(17) (2024)	EPS waste triturated	0.3% by mass	Date palm fiber	852 – 925	0.27 – 0.38

ρ – Density; λ – Thermal conductivity.

Considering the results obtained by other researchers presented in Table 1 and knowing that for a traditional gypsum material with medium hardness, the thermal conductivity is estimated to be between 0.30 - 0.43 W/m·K (18), the beneficial effect of integrating EPS waste into its matrix to improve the thermal properties and energy efficiency can be appreciated. Additionally, other advantages have been observed, such as improved acoustic insulation (16), greater resistance to water (12), and a potential source of competitive cost advantage linked to reduced fuel consumption when transporting these prefabricated products and shorter on-site installation time (19). However, all authors agree on the decrease in mechanical properties that occurs in gypsum composites when these secondary raw materials are added (20). This has led to the study of new ways of integrating the residue into the matrix, with the addition in dissolution form offering the best mechanical performance (21). However, to avoid brittle fracture of the manufactured composites and to be competitive in the market, it is necessary to incorporate reinforcing fibers to improve the ductility and increase the flexural strength of lightweight gypsum precast elements (7).

This work presents the novelty of developing a lightweight gypsum composite that integrates EPS waste in solution homogeneously in its matrix, while reinforced with synthetic polypropylene fibers (PPF). PPFs are widely used in the construction sector due to their good cost effectiveness, recyclability, lightness and high strength (22, 23). Although these fibers can be integrated in layers within precast products or used to coat them externally, they are most found randomly dispersed in the matrix (24). While there is no consensus on the optimum amount of fiber to be added to gypsum composites during the mixing process, it is known that percentages above 3% by volume negatively impact

the mechanical properties (25). The same applies when using long fibers (greater than 24 mm), which disperse poorly in the composite matrix and have a detrimental effect (26). In general terms, the addition of fibers with lengths between 6 mm and 12 mm in percentages of 0.5% and 1.0% by weight is considered to improve the flexural strength of gypsum composites (27). In addition, PPFs show good integration into the gypsum composite, adhering well to the matrix after setting (28). Their use has also been beneficial in improving the thermal resistance of gypsum precast elements (26), increasing the high temperature resistance and energy absorption capacity of these composites (29).

Therefore, it is understood that the combined effect of both materials (EPS waste and PPF) can positively impact on the development of new prefabricated products for lightweight construction, allowing progress towards greater energy efficiency in buildings. This work focuses on developing a new gypsum-based material, light-weighted with EPS in solution and reinforced with polypropylene fibers. The aim is to analyze the thermal behavior of this new material and its main physical-mechanical properties to promote its application in the construction sector. The idea arises with the intention of improving the energy efficiency of traditional gypsum composites, while maintaining good mechanical performance for use in the manufacture of prefabricated products and analyzing their behavior against fire.

2. MATERIALS AND METHODS

2.1. Materials

The following raw materials have been used for the composite production:

- Construction gypsum designated as B1 according to EN 13279-1 (30). Its main characteristics, provided by the supplying company (Saint-Gobain Placo Ibérica S.A., Spain), are the following: grain size between 0-0.2 mm, purity index of 80%, reaction to fire Euroclass A1, pH > 6.0, flexural strength ≥ 1 MPa and compressive strength ≥ 2 MPa. On the other hand, an X-ray diffraction test on this raw material showed that the most intense diffraction peaks occurred at angles of 2Θ = 14.75°, 25.66°, 29.70°, 31.856° and 49.3°, which allows classifying this material as gypsum hemihydrate ($CaSO_4 \cdot ½H_2O$).
- Drinking water from Canal de Isabel II (Madrid, Spain), with pH between 7.5-8.0, average $CaCO_3$ content of 25 mg/L and chlorine between 1.0-1.5 mg/L. The quality of this water complies with the specifications of European Council Directive 98/83/EC (31) for water for human consumption.
- EPS waste from construction and demolition waste collected directly on site. This waste was manually cut into 50 mm diameter pieces for proper handling in the laboratory. This type of insulation material has the following properties: thermal conductivity 0.037 W/m·K, density between 15-20 kg/m^3, reaction to fire Euroclass E and compressive strength 0.06 MPa.
- Universal solvent supplied by the company Nazza (Spain), composed of volatile hydrocarbons. This colorless liquid has a specific gravity of 0.85 ± 0.05 gr/cm^3, vapor pressure 85.5 mmHg and flash point of -8 °C.
- The polypropylene fibers (PPF) used are monofilament fibers with a length of 6 mm, manufactured by Sika S.A. (Spain) according to EN 14889-2 (32). Their main properties are: density 910 kg/m^3, melting point 163 °C and specific tensile strength 31.9 cN/tex.

2.2. Sample preparation

The methodology followed in the preparation of the composites is indicated in EN 13279-2:2014 (33). The water/binder ratio was obtained by means of the shaking table test, set at 0.65 to obtain a plastic consistency. In this research, two series of composites were made, one series with the incorporation of dissolved EPS waste, and another series with the addition of PPF as reinforcement. The mixtures for the series are listed in Table 2.

For the preparation of the composites, PPF was manually dispersed into the powdered binder, ensuring an adequate distribution of the fibers in the mixture. While the EPS residues were dissolved in the universal solvent with a 1:2 ratio (EPS/solvent), resulting in a liquid with density of 660 kg/m^3. This dissolution was incorporated at the end of the mixing process, obtaining a homogeneous mixture. it should be noted that the handling of solvents must be conducted in gas extraction chambers that enable air extraction and treatment, thus avoiding the release of harmful gases into the environment. The use of personal protective equipment during the handling is also recommended.

Finally, the prepared test samples were stored in a laboratory condition (23 ± 2 °C and 50 ± 5% relative humidity) for seven days. Prior to testing, the samples were dried in a stove for 24 hours at 40 ± 2 °C and 50 ± 5% relative humidity.

Table 2. Used mixtures in the production of gypsum composites

Composite	Gypsum (g)	Water (g)	PPF (g)	EPS solution (g)	Raw material saving (%)
G0.65	1000	650	—	—	—
G0.65-100	940	610	—	100	6.1
G0.65-200	879	571	—	200	12.1
G0.65-300	818	532	—	300	18.2
G0.65-PPF	1000	650	10	—	—
G0.65-100-PPF	940	610	10	100	6.1
G0.65-200-PPF	879	571	10	200	12.1
G0.65-300-PPF	818	532	10	300	18.2

PPF – Polypropylene fibers; EPS – Expanded polystyrene.

As shown in Table 2, the preparation of the composites involved reducing the amount of gypsum and water typically used in the production of gypsum materials, in favor of the incorporation of EPS waste. This approach promotes recycling and reduces the consumption of natural raw materials. The replacement was carried out progressively until reaching 18.2% incorporation of recycled material.

2.3. Experimental program

2.3.1. Mechanical characterization

- **Surface hardness**. This test was performed with a Shore C durometer on three samples of 40×40×160 mm^3 for each mixture, according to EN 13279-2:2014 (33). A distance of 20 mm was left between measurements, taking a total of 10 measurements per sample.
- **Flexural strength**. In this test, a vertical force is applied perpendicular to the sample on its longitudinal side. For this purpose, an AUTOTEST 200-10SW press (Ibertest) was used in accordance with EN 13279-2:2014 (33). Three 40×40×160 mm^3 samples were tested for each mixture.
- **Compressive strength**. Using the above-mentioned test equipment and test standards, a perpendicular force is applied over an area of 40×40 mm^2, on a total of 6 samples per mixture.
- **Scanning electron microscopy (SEM)**. Images of the samples were taken by SEM methodology with a Jeol JSM-820 microscope, operating at 20 kV, equipped with Oxford EDX analysis. The samples were prepared ensuring the inalterability of their surface.
- **X-ray diffraction**. A Siemens Krystalloflex D5000 device was used, equipped with a Cu-Kα graphite monochromator. The diffractogram was obtained in a range between $5^\circ \leq 2\theta \leq 60^\circ$ every 0.04˚, 4 seconds per-step. The sample of the hardened composites of mass 40 mg were crushed and sieved to a particle size of less than 0.3 mm. The crystallite size was calculated using the Scherrer equation (34), with Scherrer constant of 0.94 and a wavelength of 0.154056 nm for the Cu-Kα radiation source and calculating the full width at half maximum (FWHM) of the most intense peaks.

2.3.2. Thermal behavior

- **Bulk density**. This property was obtained according to UNE 102042:2023 (35), using a precision balance with 0.01 g accuracy and a caliper with 0.01 mm accuracy. For each mixture, three 40×40×160 mm^3 samples were used.
- **Thermal conductivity**. In this test, a λ-Meter EP500e equipment was used, with 150×150×30 mm^3 samples. The thermal conductivity of the composites was measured after reaching a stationary regime according to the EN 12664 standard (36).
- **Finite elements simulation**. The thermal behavior of three different construction systems (system I: lightweight interior partition, system II; light steel frame for facades, system III: lightweight cladding on a brick wall) in which the prefabricated gypsum panels, made from the gypsum composites developed, has been analyzed. Numerical 2D simulations were performed using THERM software. The simulation considered the surface thermal resistances of indoor (0.13 $m^2 \cdot K/W$) and outdoor (0.04 $m^2 \cdot K/W$) wall sides, as indicated by the Spanish CTE DB-HE/1 standard (37).

2.3.3. Fire performance

- **Direct fire**. The response of the composites to a real direct fire was evaluated following the non-standardized test proposed by Serrano Somolinos in his doctoral thesis (38), which has been carried out in previous research (39). In this test, the fuel used was 20 kg of pine wood, on which a grid with the 250×90×25 mm^3 samples was placed. During the 25-minute test, the surface temperature of the samples was recorded every five minutes with a Testo 845 infrared thermometer and thermographic images with a FLIR E40bx camera. Fire curves, accumulated energy in the composites and mass loss experienced by the test samples were determined for each mixture.
- **Thermogravimetric analysis (TGA)**. The samples were subjected to a thermal process, starting from room temperature up to 1000°C, at 10°C/minute. An SDT Q600 (TA Instruments) was used in a controlled air atmosphere with a flow rate of 100 ml/min. Platinum sample cups with a capacity of 110 µL were used for the test. The analysis was performed on a sample of approximately 40-50 mg. Prior to the test, the samples were ground in an agate mortar and sieved with a 0.3 mm mesh aperture sieve.
- **Determination of toxic emissions**. Theoretical emissions of carbon monoxide and carbon dioxide produced during the combustion of a false ceiling in a standard room of 3×4×2.6 m^3, made with the composites developed in this research, were measured. For this purpose, the total organic carbon (TOC) and inorganic carbon (IC) content was analyzed using a LECO TruSpec Macro CHN unit in a controlled atmosphere of O_2.

3. RESULTS AND DISCUSSION

3.1. Mechanical characterization

The results for hardness, flexural strength and compressive strength of the produced composites are shown in Figure 1. The obtained results have been compared with the reference values in each series.

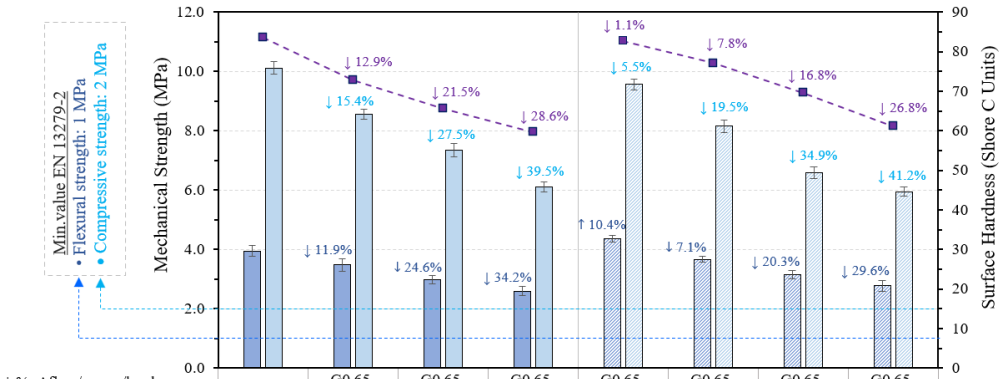

↓ %: Δflex./comp./hardness vs G0.65	G0.65	G0.65-100	G0.65-200	G0.65-300	G0.65-PPF	G0.65-100-PPF	G0.65-200-PPF	G0.65-300-PPF
Flexural Strength	3.95	3.48	2.98	2.60	4.36	3.67	3.15	2.78
Compressive Strength	10.12	8.56	7.34	6.12	9.56	8.15	6.59	5.95
Superficial Hardness	83.6	72.8	65.6	59.7	82.7	77.1	69.6	61.2

Figure 1. Flexural strength, compressive strength and surface hardness of gypsum composites.

Figure 1 shows the decrease in surface hardness of the composites as the amount of dissolved EPS in their composition increases, with composite G0.65-300 showing the greatest reduction (28.6%). The addition of PPF by itself slightly decreased this property. However, in the composites containing EPS, the fibers showed a positive impact increasing the hardness with respect to the counterpart composites without fibers by 1.8%-5.1%.

The flexural and compressive strengths followed a similar trend, decreasing proportionally to the amount of dissolved EPS added. The reduction in mechanical strength when incorporating recycled lightweight additions, such as EPS or XPS, is common in this type of composite, as these materials have a lower density than the gypsum material itself, generating a more porous composite (20). Nevertheless, the values achieved in this research comply with the current applicable regulations. The composites with PPF exhibited a significant improvement in flexural strength, reducing the effect of the dissolved EPS addition by 4.6%-4.8%. On the other hand, the compressive strength of the composites decreased when fibers were incorporated, with the most unfavorable composite being G0.65-300-PPF. Similar results were observed when mineral wool fibers were incorporated into mortars, with the compressive strength progressively decreasing as the density of the composites reduced (40).

The SEM images obtained for G0.65 and G0.65-300-PPF composites reveal the main differences caused by the additions proposed in this research in the internal microstructure of the material and provide further insight into its mechanical behavior (Figure 2). The samples for this test were extracted from the composites' interior, avoiding damaging their surface and capturing the most representative information.

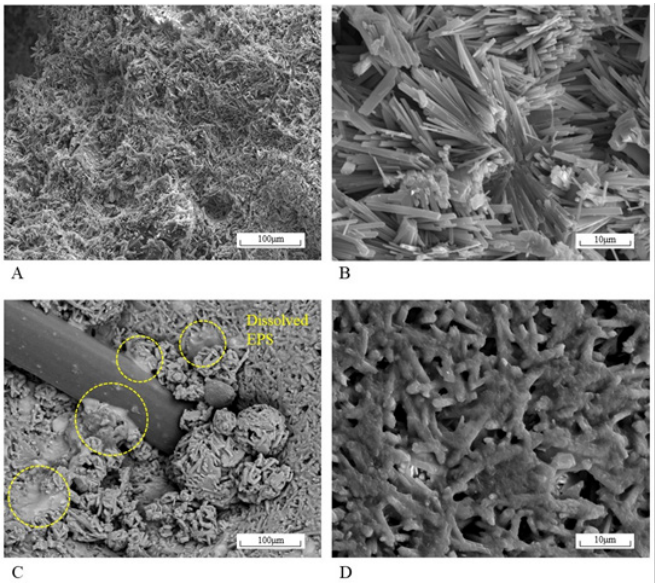

Figure 2. SEM images. A: G0.65 composite, ×500; B: G0.65 composite, ×2000; C: G0.65-300-PPF composite, ×500; D: G0.65-300-PPF composite, ×2000.

As seen in Figure 2A, the matrix of the reference composite G0.65 appears generally homogeneous and compact, although some pores formed during the hydration of the hemihydrate can be observed. At higher magnification (x2000), in Figure 2B, the characteristic acicular crystals of the gypsum mineral can be seen, oriented in all directions, which densifies the interior of the material (41).

In contrast, in the G0.65-300-PPF composite (Figure 2C), some disaggregation is observed in the matrix caused by the incorporation of the dissolved EPS. This addition is able to insert itself into the free voids between crystals and even coat them as a superficial film, which disrupts the crystalline structure and weakens the material. As can be seen in Figure 2D, the dissolved EPS thickens and shortens the gypsum crystals, which also decreases the mechanical strength of the composite (12). Figure 2C shows the good bond formed between the PPF and the matrix, which corroborates the positive performance observed in the mechanical properties of the composites incorporating them (13).

Furthermore, as can be seen in Figures 2B and 2D, the incorporation of the EPS dissolution causes a variation in the crystalline structure within the gypsum composite matrix. In this sense, the growth of the dihydrate crystals can be conditioned by the inclusion of this recycled material, leading to a decrease in mechanical strength (21), as observed in Figure 1. Therefore, an X-ray diffraction analysis of the composites has been performed as the recycled material content increases (Figure 3) and the crystallite size in each sample has been calculated for the peak of highest intensity (Table 3).

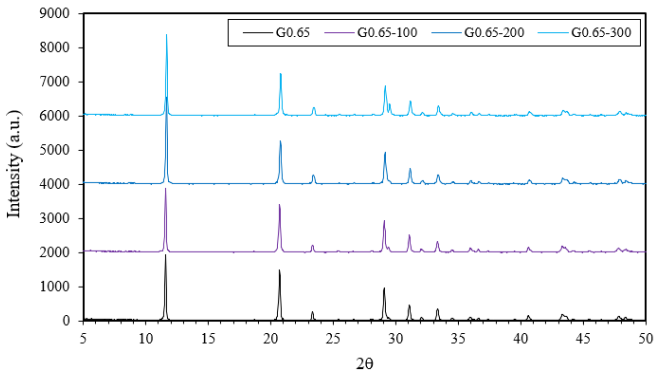

Figure 3. Diffractogram of the different gypsum composites. The peaks correspond to the dihydrate crystals ($CaSO_4 \cdot 2H_2O$).

Table 3. Mean size (D) of the ordered crystalline domains of the samples (2Θ = 11.65°).

Sample	Peak position (degree)	B = FWHM (degree)	Crystallite size (nm)
G0.65	11.58	0.1222	68.24
G0.65-100	11.58	0.1290	64.67
G0.65-200	11.58	0.1333	62.54
G0.65-300	11.58	0.1308	63.77

FWHM – Full width at half maximum.

Figure 3 shows that the diffractograms corresponding to the different analyzed samples exhibit the same pattern, with peaks corresponding to gypsum dihydrate appearing in all of them. The three most intense peaks are located at diffraction angles 2Θ = 11.65°, 20.74° and 29.15° (42). Additionally, Table 3 shows the results for the crystallite size at the most intense peak (2Θ = 11.65°) of all the composites, revealing a tendency to reduce the crystallite size when incorporating EPS solution in the gypsum composites produced. The difference between samples G0.65-200 and G0.65-300 may be due to the specific sample analysed in XDR, however, in other recent research (43) it was found a trend that corroborates this aspect. This corroborates that the added dissolution modifies the microstructure as observed in the SEM analysis and is linked to the reduction of the mechanical strength compared to the reference material.

3.2. Thermal behavior

The results for thermal conductivity and bulk density, as well as their relation to the reference, are shown in Figure 4.

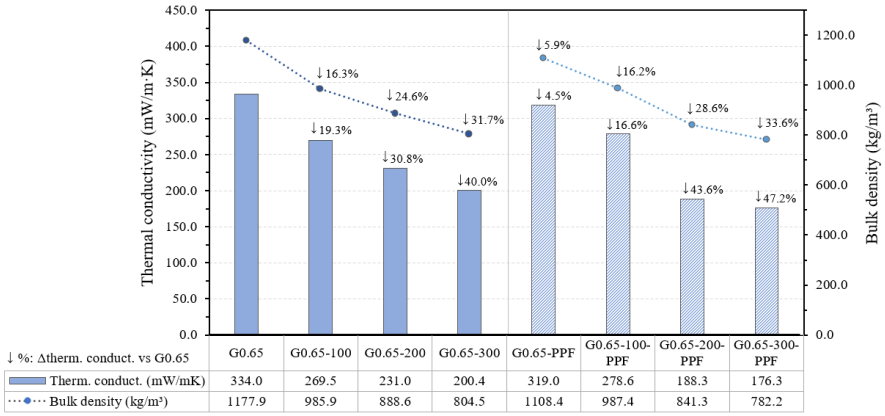

↓ %: Δtherm. conduct. vs G0.65	G0.65	G0.65-100	G0.65-200	G0.65-300	G0.65-PPF	G0.65-100-PPF	G0.65-200-PPF	G0.65-300-PPF
Therm. conduct. (mW/mK)	334.0	269.5	231.0	200.4	319.0	278.6	188.3	176.3
Bulk density (kg/m³)	1177.9	985.9	888.6	804.5	1108.4	987.4	841.3	782.2

Figure 4. Thermal conductivity and bulk density of elaborated gypsum composites.

As shown in Figure 4, the incorporation of dissolved EPS during mixing process decreases the bulk density of the hardened gypsum composites in respect to the reference (G.065). This reduction was more significant in the G0.65-300 composite (down to 31.7%) as it contained a higher proportion of recycled material. The addition of PPF resulted in a slight decrease in bulk density compared to the composites without fibers, ranging from 1.9%-5.9%. The dissolved EPS is able to contain air bubbles within the gypsum matrix, resulting in a less compact and lighter material (8, 12).

Likewise, this decrease in bulk density directly influences the thermal conductivity of the composites (44), with a clear decrease when a greater substitution of gypsum material by the EPS solution is made. In composites without fibers, this reduction is noticeably linear, with the thermal conductivity decreasing by around 10% for every 100 g of EPS solution added. The incorporation of PPF enhances this reduction, being more evident in the G0.65-200-PPF and G0.65-300-PPF composites, with values 12.8% and 7.2% lower than their counterparts without fibers, respectively. The decrease in thermal conductivity is attributed to the increased porosity of the composites, hindering heat transfer through the material (12).

A comparative graph of the bulk density and thermal conductivity of the developed composites in this research is presented in Figure 5, comparing them with other similar studies that incorporated shredded EPS or XPS in gypsum composites.
As observed in Figure 5, all gypsum composites presented in this research exhibit thermal conductivity values below the design values established by EN 13279-1 (30) in relation to the obtained densities, denoting a good thermal performance. In other studies, where lower thermal conductivities were achieved by drastically reducing the density (16, 45, 46), a significant weakening of the material occurred, even failing to meet the minimum mechanical strengths established in the standard, which not happen in the present study, as previously illustrated in Figure 1.

The heat transfer simulations using THERM software are shown in Figure 6. The analyzed composites included the reference (G0.65) and the composite with fibers and higher dissolved EPS content (G0.65-300-PPF), which showed the highest and lowest thermal conductivity, respectively. Additionally, three representative temperatures inside each system have been indicated: A, cold zone of the steel profile; B, internal point of the wall; C, hot zone of the steel stud.

Composition of the construction systems. System I and III: 1: gypsum panel (e: 15 mm; λ: shown in Figure 4), 2: mineral wool (e: 45 mm; λ: 0.035 W/m·K), 3: steel stud (e: 0.6 mm; λ: 50.000 W/m·K), 5: masonry wall (e: 70 mm; λ: 0.32 W/m·K). System II: 1: gypsum panel (e: 15 mm; λ: W/m·K), 2: mineral wool (e: 90 mm; λ: 0.035 W/m·K), 3: steel stud (e: 1.5 mm; λ: 50.000 W/m·K), 4: OSB (e: 12 mm; λ: 0.100 W/m·K)

In all the analyzed construction systems, the overall thermal resistance of the walls increased by introducing the gypsum panel made from the composites developed in this research. The thermal resistance increased by 21.1%, 7.7% and 8.7% in systems I,

II and III, respectively, when compared to using the reference gypsum panel. The results obtained demonstrate the significant potential of the new material proposed in this study to enhance energy efficiency in buildings, especially in partitions of reduced thickness and low thermal inertia, which is one of the main applications of prefabricated gypsum panels in construction (47).

The temperatures indicated in Figure 6 show that in System I, the thermal gradient between cold and warm sides is reduced by up to 2.6°C with respect to the reference, helping to control interstitial condensation more effectively. In systems II and III, the greater thicknesses of the component layers limit the contribution of the G0.65-300-PPF composite, although there is still a reduction in the thermal gradient of 0.7-1.0°C. It is worth noting the considerable increase in thermal resistance of these building systems only by varying the material of 15 mm internal finishing layer.

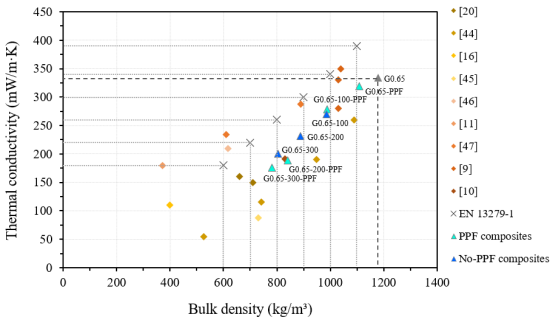

Figure 5. Bulk density vs thermal conductivity of the developed composites in relation to other studies.

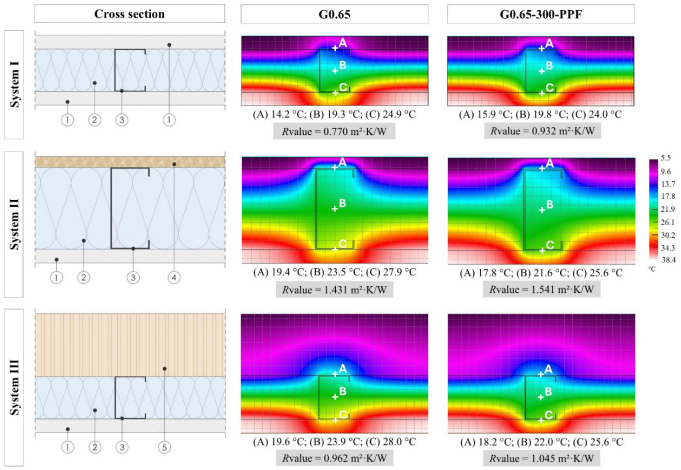

Figure 6. Construction details and temperature distribution of the simulated models.

3.3. Fire performance

Figure 7 illustrates the setup of the test samples during the direct fire behavior test. Figure 8 presents the time-temperature curve obtained from the direct fire test for the composites developed in this research. The average surface temperature of the samples at the beginning of the test was 18.4°C.

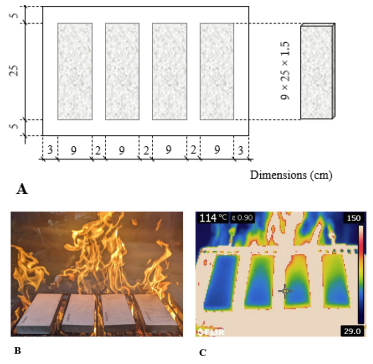

Figure 7. Direct fire test. A: sample setup during the test; B: photograph of the samples subjected to fire; C: thermographic image taken during the test.

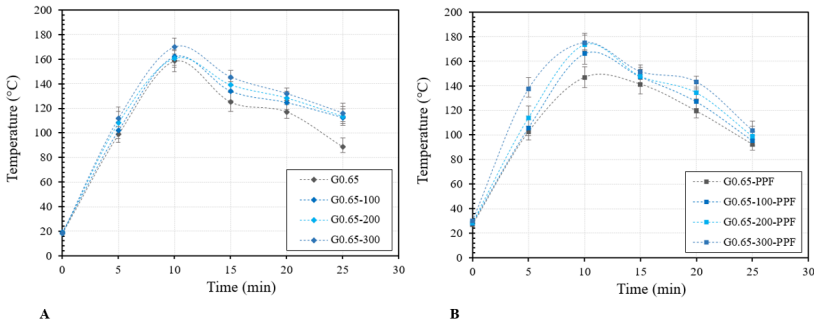

Figure 8. Time-temperature curves obtained. A: composites without PPF, B: composites with PPF.

As shown in Figure 8, the highest temperature rise occurs during the first five minutes of the test, reaching the maximum temperature after ten minutes. In the unreinforced composites, the reference sample G0.65 reached the lowest peak temperature (158 °C). However, as the amount of dissolved EPS in the composites increased, this peak temperature also rose (up to 169.8 °C in composite G0.65-300). This increase in surface temperature of the samples with dissolved EPS is due to the onset of thermal degradation of the polymer within the gypsum matrix (around 100 °C), which undergoes its glass transition at 130 °C (48). At the end of the test, the composites with EPS retained a higher temperature compared to the reference (around 25°C), with no significant differences in the amount of EPS added.

The combination of dissolved EPS and PPF resulted in a general increase in the recorded surface temperatures of the composites, as the melting point of the fibers (163°C (38)) contributed to a higher energy accumulation in the samples.

The highest temperature recorded in this series was in G0.65-300 composite (175°C). By the end of the test, all the composites in this series with PPF obtained similar temperatures, around 98°C.

Table 4. Fire severity during direct fire test and mass loss of composites.

Composite	Fire Severity (°C·min)	Δ mass (%)	Composite	Fire Severity (°C·min)	Δ mass (%)
G0.65	2763.6	8.8	G0.65 PPF	2826.4	7.4
G0.65-100	2940.1	12.0	G0.65-100-PPF	3016.3	11.6
G0.65-200	3007.3	13.4	G0.65-200-PPF	3142.4	12.2
G0.65-300	3128.0	14.3	G0.65-300-PPF	3336.8	12.8

Table 4 shows the fire severity experienced by the composites, which corresponds to the area under the time-temperature curve of the direct fire test, as well as the observed mass loss.

As can be seen in Table 4, the fire severity increased as the proportion of dissolved EPS replaced the gypsum material in the composites, ranging from 6%-13% compared to the reference G0.65. The addition of PPF slightly raised these values, by 2% to 7% with respect to the equivalent composites without fibers. On the other hand, mass loss increased in the composites with dissolved EPS up to 5.5% in sample G0.65-300. However, the addition of PPF as reinforcement moderately reduced this mass loss. As indicated by Serrano et al. (38), the melting of PPF creates free channels within the gypsum matrix, facilitating the release of vapor and increasing the material's stability.

Table 5 presents the main TGA results for the prepared composites. The sample preparation process (crushing and sieving) in this test prevents the preservation of the PPFs in the samples, so only the composites incorporating dissolved EPS were analyzed.

Table 5. Summary table of the thermogravimetric analysis of compounds G0.65, G0.65-100, G0.65-200 and G0.65-300.

Sample	Total mass loss (%)	Interval (°C)	Maximum temperature (°C)	Partial mass loss (%)	Associated heating effects	Comments
G0.65	22.07	< 200	127.83	17.0	Endothermal	DH to HH
			138.59		Endothermal	HH to anhydrite
		200-550	357.12	-	Exothermal	Anhydrite phase transition
		500-800	703.4	4.4	Endothermal	$CaCO_3$ to CaO
G0.65-100	25.58	< 200	129.18	16.1	Endothermal	DH to HH
			142.62		Endothermal	HH to anhydrite
		200-550	383.34; 476.8	4.8	Exothermal	EPS combustion
		550-800	709.45	4.5	Endothermal	$CaCO_3$ to CaO
G0.65-200	29.45	< 200	127.16	15.9	Endothermal	DH to HH
			136.57		Endothermal	HH to anhydrite
		200-550	386.70; 470.08	9.6	Exothermal	EPS combustion
		550-800	696.68	3.9	Endothermal	$CaCO_3$ to CaO
G0.65-300	30.03	< 200	128.5	14.9	Endothermal	DH to HH
			136.57		Endothermal	HH to anhydrite
		200-550	376.62; 466.72	13.6	Exothermal	EPS combustion
		550-800	698.69	3.9	Endothermal	$CaCO_3$ to CaO

DH: calcium sulphate dihydrate; HH: calcium sulphate hemihydrate.

As shown in Table 5, the reference sample G0.65 experiences a total mass loss of 22.1%. In the first temperature interval, up to 200°C, an endothermic process occurs, leading to the first major mass loss of up to 17.0% of the total mass. The highest mass loss rate occurs at 127.83°C, corresponding to the transformation of dihydrate calcium sulphate ($CaSO_4$-$2H_2O$) into hemihydrate calcium sulphate ($CaSO_4$-$0.5H_2O$). A second peak appears with a maximum temperature of 138.59°C, where hemihydrate calcium sulphate is completely dehydrated, resulting in anhydrous calcium sulphate or anhydrite ($CaSO_4$). Subsequently, in the temperature range from 200°C to 550°C, an exothermic event occurs, peaking at 357.12°C. Since this process has no associated mass loss, it corresponds to the phase change from anhydrite α to anhydrite β. Finally, in the temperature range from 550°C to 800°C, another mass loss (4.4%) occurs in an endothermic process, with a maximum mass loss rate at 703.4°C. This last event is associated with the thermal decomposition of calcium carbonate ($CaCO_3$), present in the gypsum raw material, into calcium oxide (CaO).

As observed in Table 5, in the other composites, the total mass loss progressively increases with the amount of EPS incorporated, reaching up to 30.0% in the sample with the highest EPS content (G0.65-300). Samples containing EPS exhibit additional thermal events related to the presence of the polymer. Thus, in sample G0.65-100 an exothermic thermal event is observed in the temperature range from 250°C to 550°C, with a maximum mass loss rate occurring

around 383°C and a lesser intensity around 477°C. This event, with a mass loss of 4.8%, corresponds to the combustion of the EPS contained in the samples (49).

The thermal event associated with the phase transformation from anhydrite α to β in the samples containing EPS is masked by the combustion of EPS, since they occur in the same temperature range. Samples G0.65-200 and G0.65-300 show similar temperature behavior, with mass loss associated with EPS combustion being higher at 9.6% and 13.6%, respectively, due to the greater amount of polystyrene in their formulation.

The emissions calculation has been performed for samples G0.65, G0.65-100, G0.65-200 and G0.65-300 (Table 6) since the main objective of this test is to know the potential contribution of EPS to the total emissions computation. In addition, it should be considered that the small amount of fibers added to the composites would not significantly increase the results obtained.

Table 6. Results of total carbon analysis of composites.

Sample	Analyzed mass (mg)	Total carbon (%)	Inorganic carbon (%)	Organic carbon (%)
G0.65	100	1.4	1.33	0.07
G0.65-100	100	5.07	1.32	3.75
G0.65-200	100	9.28	1.34	7.94
G0.65-300	100	13.16	1.39	11.77

Table 7. Estimation of emitted CO_2 and CO in the combustion of false ceiling made with the compounds G0.65, G0.65-100, G0.65-200 and G0.65-300 in a standard room of 12 m^2.

Composite	Bulk density (kg/m^3)	Plate mass (kg)	CO_2 emitted (kg)	CO emitted (kg)	CO_2 emitted (ppm)	CO emitted (ppm)
G0.65	1177.90	14.72	0.45	0.29	14.53	9.25
G0.65-100	985.90	12.32	20.33	12.94	651.74	414.74
G0.65-200	888.60	11.11	38.81	24.69	1243.76	791.48
G0.65-300	804.50	10.06	52.08	33.14	1669.21	1062.22

As seen in Table 6, and as would be expected based on the composition of the samples, the total organic content of the sample increases as the EPS content rises; this result is also consistent with the thermal analysis for the mass loss in the 200-550°C range, associated with EPS combustion. The inorganic carbon content is related with the presence of calcium carbonate in the samples, and remains approximately constant across all samples, aligning with the thermal analysis results for mass loss between 550 and 800°C. The increase in organic carbon is similar to other studies where polymeric materials have been added to the composites (39).

In addition, the estimation of CO and CO_2 emissions that would be released during the fire of a false ceiling made with the composites developed in this research has been carried out and is presented in Table 7.

As shown in Table 7, the incorporated EPS dissolution generates a significant increase in CO and CO_2 emissions as the proportion of the recycled waste in the composites increases. These results are expected due to the organic nature of the composites, as previously discussed in the carbon analysis. Likewise, the concentrations of each gas also increase in the same proportion, although in no case, do they exceed 40000 ppm for CO_2 and 2000 ppm for CO, which are considered immediately dangerous to life or health (IDLH) values by the material safety data sheet (MSDS) (50).

It should be noted that the CO and CO_2 obtained would correspond to either complete or incomplete combustion respectively, which is an unlikely scenario. In a real situation, it is usual that a combination of both types of combustion would occur, and therefore lower amounts of each of these gases would be generated.

4. CONCLUSIONS

In this research, the mechanical, thermal and fire performance of a new gypsum composite incorporating EPS waste in solution and PPF as reinforcement has been studied. Additionally, the development of this composite was approached with a focus on sustainability, through the partial substitution of original natural raw materials with recycled materials. The obtained results allow the following main conclusions to be drawn:

- Composites that include dissolved EPS in their composition experience a significant reduction in their mechanical strength. SEM images and gypsum crystal size analysis show how the inclusion of recycled material affects the crystal morphology, weakening the matrix. The inclusion of PPF largely mitigates this reduction by improving the flexural strength. It is noteworthy that all the obtained values are above the minimum requirements set by the current regulations.
- The newly developed gypsum composites show a significant reduction in thermal conductivity and density, which increases the thermal resistance of construction systems that incorporate them as finishing layer. Specifically, their effect is much more pronounced in systems with reduced thickness and thermal inertia, thereby contributing to the energy efficiency of buildings.
- The developed gypsum composites exhibit an increase in surface temperature when exposed to fire. The polymer added to the matrix promotes mass loss after exposure, with the composites incorporating PPF showing better stability under fire action. The organic nature of the added material increases the amount of toxic gases released during a fire. However, the obtained values are below those established by IDLH limits.

It should be noted that in this research the hygrothermal characterization of the developed composites has not been carried out, nor how the variation of the environmental moisture content could affect the thermal performance of the material. However, this limitation raises a future line of research on these new materials.

The environmental impact that the use of organic solvents can have must also be considered, so life cycle analysis of these compounds will be of great interest in future research, allowing more sustainable alternatives to be proposed. Moreover, this analysis would allow us to identify weak points of the process and propose improvements in their production. In this sense, the redesign of prefabricated construction products such as gypsum-based boards or panels makes it necessary to rethink the recycling process to obtain Cradle to Cradle certification. While it is true that the incorporation of these recycled raw materials can have a lower environmental impact during the use phase of the product, it can also hinder the recyclability of the material by increasing the complexity of separating the original raw materials.

Acknowledgements

The authors would like to acknowledge the University of Malaga for their help in the analysis of the fire tests. This research was funded by Madrid Government (Comunidad de Madrid-Spain) under the Multiannual Agreement 2023-2026 with Universidad Politécnica de Madrid in the Line A, Emerging PhD researchers, grant number DOCTORES-EMERGENTES-24-NZMO4U-16-3U7Z8W (Name of the project: Waste2BuildIns; reference OTT: M230020126A-DFV).

Authorship contribution statement

Alicia Zaragoza: Data Curation, Formal analysis, Investigation, Methodology, Software, Visualization, Writing-original draft.

Daniel Ferrández: Conceptualization, Data Curation, Formal analysis, Funding acquisition, Investigation, Project administration, Resources, Supervision, Validation, Writing - original draft.

Paulo Santos: Data Curation, Formal analysis, Investigation, Methodology, Supervision, Validation, Writing - review & editing.

Evangelina Atanes-Sánchez: Data Curation, Formal analysis, Investigation, Methodology, Software, Writing - original draft.

Declaration of competing interest

The authors of this article declare that they have no financial, professional or personal conflicts of in-terest that could have inappropriately influenced this work.

REFERENCES

1. D'Agostino D, Congedo PM, Albanese PM, Rubino A, Baglivo C. 2024. Impact of climate change on the energy performance of building envelopes and implications on energy regulations across Europe. Energy. 288:129886. https://doi.org/10.1016/j.energy.2023.129886
2. Marincu C, Dan D, Moga L. 2024. Investigating the influence of building shape and insulation thickness on energy efficiency of buildings. Energy Sustain. Dev. 79:101384. https://doi.org/10.1016/j.esd.2024.101384
3. Mucedero G, Monteiro R. 2024. An integrated regional prioritisation framework for seismic and energy-efficiency performance upgrading of residential buildings. Int. J. Disaster Risk Reduct. 103:104341. https://doi.org/10.1016/j.ijdrr.2024.104341
4. Zaragoza-Benzal A, Ferrández D, Santos P, Cunha A, Durães L. 2024. Recovering low-density polyethylene waste for gypsum board production: a mechanical and hygrothermal study. Materials. 17(16):3898. https://doi.org/10.3390/ma17163898
5. Pedreño-Rojas MA, Fořt J, Černý R, Rubio-de-Hita P. 2020. Life cycle assessment of natural and recycled gypsum production in the Spanish context. J. Clean. Prod. 253. https://doi.org/10.1016/j.jclepro.2020.120056
6. Doleželová M, Krejsová J, Scheinherrová L, Keppert M, Vimmrová A. 2022. Investigation of environmentally friendly gypsum based composites with improved water resistance. J. Clean. Prod. 370:133278. https://doi.org/10.1016/J.JCLEPRO.2022.133278
7. Balti S, Boudenne A, Yahya K, Hamdi N. 2024. Advancing reinforcement of sustainable gypsum composites: High-performance design by reusing waste materials. Mater. Today Sustain. 27:100946. https://doi.org/10.1016/j.mtsust.2024.100946
8. Río-Merino M del, Vidales-Barriguete A, Piña-Ramírez C, Vitiello V, Santa Cruz-Astorqui J, Castelluccio R. 2022. A review of the research about gypsum mortars with waste aggregates. J. Build. Eng. 45:103338. https://doi.org/10.1016/j.jobe.2021.103338
9. Villoria Sáez P, Río Merino M del, Sorrentino M, Amores CP, Cruz Astorqui JS, Viñas Arrebola C. 2020. Mechanical characterization of gypsum composites containing inert and insulation materials from construction and demolition waste and further application as a gypsum block. Materials. 13(1):193 https://doi.org/10.3390/MA13010193

10. Bouzit S, Merli F, Sonebi M, Buratti C, Taha M. 2021. Gypsum-plasters mixed with polystyrene balls for building insulation: Experimental characterization and energy performance. Constr. build. mater. 283: 122625. https://doi.org/10.1016/J.CONBUILDMAT.2021.122625
11. Oliveira KA de, Oliveira CAB, Molina JC. 2021. Lightweight recycled gypsum with residues of expanded polystyrene and cellulose fiber to improve thermal properties of gypsum. Mater. de Construcc. 71(341):242–242. https://doi.org/10.3989/MC.2021.07520
12. López Pedrajas D, Carmona Franco M, Garrido Sáenz I, Ramos Mellado FJ, Rodríguez Romero JF, Borreguero Simón AM. 2022. Polystyrene nanoparticles slurry as an additive for developing insulating and waterproof gypsum composites. Appl. Therm. Eng. 217:119271. https://doi.org/10.1016/J.APPLTHERMALENG.2022.119271
13. Bumanis G, Sapata A, Sinka M, Spurina E, Bajare D. 2023. Additive manufacturing of lightweight gypsum and expanded polystyrene granulate composite. Journal of composites scienc. 7(10):425. https://doi.org/10.3390/jcs7100425
14. Bumanis G, Argalis PP, Sahmenko G, Mironovs D, Rucevskis S, Korjakins A, Bajare D. 2023. Thermal and sound insulation properties of recycled expanded polystyrene granule and gypsum composites. Recycling. 8(1):19. https://doi.org/10.3390/recycling8010019
15. Zaragoza-Benzal A, Ferrández D, Atanes-Sánchez E, Saíz P. 2023. Dissolved recycled expanded polystyrene as partial replacement in plaster composites. J. Build. Eng. 65:105697. https://doi.org/10.1016/j.jobe.2022.105697
16. Jin Z, Cui C, Wan Z, Su Y, He X, Ma B, Zhi Z, Chen S, Wang B. 2023. Preparation of eco-friendly functional lightweight gypsum: Effect of three different lightweight aggregates. Constr. Build. Mater. 400:132875. https://doi.org/10.1016/j.conbuildmat.2023.132875
17. Benchouia HE, Boussehel H, Guerira B, Sedira L, Tedeschi C, Becha Hossam E, Cucchi M. 2024. An experimental evaluation of a hybrid bio-composite based on date palm petiole fibers, expanded polystyrene waste, and gypsum plaster as a sustainable insulating building material. Constr. Build. Mater. 422:135735. https://doi.org/10.1016/j.conbuildmat.2024.135735
18. Ministerio de Vivienda - Gobierno de España. Catálogo de elementos constructivos del CTE. 2010.
19. Zaragoza-Benzal A, Ferrández D, Diaz-Velilla JP, Zúñiga-Vicente JA. 2023. Manufacture and characterisation of a new lightweight plaster for application in wet rooms under circular economy criteria. Case Stud. Constr. Mater. 19:e02380. https://doi.org/10.1016/j.cscm.2023.e02380
20. Rio Merino M del, Villoria Sáez P, Longobardi I, Santa Cruz Astorqui J, Porras-Amores C. 2019. Redesigning lightweight gypsum with mixes of polystyrene waste from construction and demolition waste. J. clean. prod. 220:144–151. https://doi.org/10.1016/J.JCLEPRO.2019.02.132
21. Zaragoza-Benzal A, Ferrández D, Santos P, Atanes-Sánchez E. 2024. Development and characterization of new lightweight waste-based plaster composites for building applications. J. Build. Eng. 96:110525. https://doi.org/10.1016/j.jobe.2024.110525
22. Pekrioglu Balkis A. The effects of waste marble dust and polypropylene fiber contents on mechanical properties of gypsum stabilized earthen. 2017. Constr. Build. Mater. 134:556–562. https://doi.org/10.1016/j.conbuildmat.2016.12.172
23. Flores Medina N, Barbero-Barrera MM. Mechanical and physical enhancement of gypsum composites through a synergic work of polypropylene fiber and recycled isostatic graphite filler. 2017. Constr. Build. Mater. 131:165–177. https://doi.org/10.1016/j.conbuildmat.2016.11.073
24. Durgun MY. Effect of wetting-drying cycles on gypsum plasters containing ground basaltic pumice and polypropylene fibers. 2020. J. build. eng. 32:101801. https://doi.org/10.1016/J.JOBE.2020.101801
25. Zhu C, Zhang J, Peng J, Cao W, Liu J. Physical and mechanical properties of gypsum-based composites reinforced with PVA and PP fibers. 2018. Constr. Build. Mater. 163:695–705. https://doi.org/10.1016/j.conbuildmat.2017.12.168
26. Álvarez M, Ferrández D, Morón C, Atanes□Sánchez E. Characterization of a New Lightened Gypsum-Based Material Reinforced with Fibers. 2021. Materials. 14(5):1203. https://doi.org/10.3390/MA14051203
27. Li Z, Wang X, Yan W, Ding L, Liu J, Wu Z, Huang H. 2023. Physical and mechanical properties of gypsum-based composites reinforced with basalt, glass, and PVA fibers. J. Build. Eng. 64:105640. https://doi.org/10.1016/J.JOBE.2022.105640
28. Romero-Gómez MI, Pedreño-Rojas MA, Pérez-Gálvez F, Rubio-de-Hita P. 2021. Characterization of gypsum composites with polypropylene fibers from non-degradable wet wipes. J. Build. Eng. 34: 101874. https://doi.org/10.1016/j.jobe.2020.101874
29. Romero-Gómez MI, Silva R V., Flores-Colen I, Brito J de. 2023. Physico-mechanical properties of plastic waste-containing gypsum composites exposed to elevated temperature. Constr. Build. Mater. 398: 132530. https://doi.org/10.1016/j.conbuildmat.2023.132530
30. AENOR. UNE-EN 13279-1, Gypsum binders and gypsum plasters. Part 1: Definitions and requirements. Madrid, Spain: 2009.
31. European Parliament and the Council. Council Directive 98/83/EC of 3 November 1998 on the quality of water intended for human consumption. 1998.
32. AENOR. UNE-EN 14889-2:2008, Fibres for concrete - Part 2: Polymer fibres - Definitions, specifications and conformity. 2008.
33. AENOR. UNE-EN 13279-2:2014, Gypsum binders and gypsum plasters - Part 2: Test methods. 2014.
34. Patterson AL. 1939. The Scherrer Formula for X-Ray particle size determination. physical review. 56(10):978–982.

35. AENOR. UNE 102042, Gypsum plasters. Other test methods. 2023.
36. AENOR. UNE-EN 12664, Thermal performance of building materials and products. Determination of thermal resistance by means of guarded hot plate and heat flow meter methods. Dry and moist products of medium and low thermal resistance. Madrid, Spain: 2002.
37. CTE DB-HE/1. 2022. Código técnico de la edificación. ahorro energético. 2022.
38. Serrano R, Cobo A, Prieto MI, González M de las N. 2016. Analysis of fire resistance of concrete with polypropylene or steel fibers. Constr. Build. Mater. 122:302–309. https://doi.org/10.1016/J.CONBUILDMAT.2016.06.055
39. Vidales-Barriguete A, Piña-Ramírez C, Serrano-Somolinos R, Río-Merino M del, Atanes-Sánchez E. 2021. Behavior resulting from fire in plasterboard with plastic cable waste aggregates. J. Build. Eng. 40:102293. https://doi.org/10.1016/j.jobe.2021.102293
40. Piña Ramírez C, Río Merino M del, Viñas Arrebola C, Vidales Barriguete A, Kosior-Kazberuk M. 2019. Analysis of the mechanical behaviour of the cement mortars with additives of mineral wool fibres from recycling of CDW. Constr. Build. Mater. 210:56–62. https://doi.org/10.1016/j.conbuildmat.2019.03.062
41. Lanzón M, Castellón FJ, Ayala M. 2022. Effect of the expanded perlite dose on the fire performance of gypsum plasters. Constr. build. mater. 346:128494. https://doi.org/10.1016/J.CONBUILDMAT.2022.128494
42. Strydom CA, Potgieter JH. 1999. Dehydration behaviour of a natural gypsum and a phosphogypsum during milling. Thermochim. Acta. 332(1):89–96. https://doi.org/10.1016/S0040-6031(99)00083-0
43. Zaragoza-Benzal A, Ferrández Daniel, Santos Paulo, Atanes-Sánchez Evangelina. 2024. Upcycling EPS waste and mineral wool to produce new lightweight gypsum composites with improved thermal performance. Constr. Build. Mater. 449: 138464. https://doi.org/10.1016/j.conbuildmat.2024.138464
44. Wang T, Gao X, Wang J. 2019. Preparation of foamed phosphogypsum lightweight materials by incorporating cementitious additives. Mater. Science. 25(3):340–347. https://doi.org/10.5755/j01.ms.25.3.19910
45. Bicer A, Kar F. 2017. Thermal and mechanical properties of gypsum plaster mixed with expanded polystyrene and tragacanth. Therm. Sci. eng. prog. 1:59–65. https://doi.org/10.1016/J.TSEP.2017.02.008
46. San-Antonio-González A, Río Merino M Del, Viñas Arrebola C, Villoria-Sáez P. 2015. Lightweight material made with gypsum and extruded polystyrene waste with enhanced thermal behaviour. Constr. Build. Mater. 93:57–63. https://doi.org/10.1016/J.CONBUILDMAT.2015.05.040
47. Zhou H, Puttige AR, Nair G, Olofsson T. 2024. Thermal behaviour of a gypsum board incorporated with phase change materials. J. build. eng. 94:109928. https://doi.org/10.1016/j.jobe.2024.109928
48. Xu Q, Jin C, Jiang Y. 2014. Analysis of the relationship between MCC and thermal analysis results in evaluating flammability of EPS foam. J. Therm. Anal. Calorim. 118:687–693. https://doi.org/10.1007/s10973-014-3736-0
49. Zhang W, Zhang J, Ding Y, He Q, Lu K, Chen H. 2021. Pyrolysis kinetics and reaction mechanism of expandable polystyrene by multiple kinetics methods. J. Clean Prod. 285:125042. https://doi.org/10.1016/j.jclepro.2020.125042
50. Dotson GS, Niemeier R. 2012. Derivation of immediately dangerous to life or health (IDLH) values.